12595

Toward Elimination of Discrepancies between Theory and Experiment: Double Proton Transfer in Dimers of Carboxylic Acids

Thomas Loerting and Klaus R. Liedl*

Contribution from the Department of Theoretical Chemistry, Institute of General, Inorganic and Theoretical Chemistry, University of Innsbruck, Innrain 52a, A-6020 Innsbruck, Austria

Received May 19, 1998. Revised Manuscript Received September 24, 1998

Abstract: We present for the first time a fully ab initio dual-level reaction path dynamics calculation of the synchronous proton exchange in carboxylic acid dimers that is consistent with a wide variety of experimental findings, such as reaction rates k, tunneling splittings Δ_0, apparent activation energy curves E_a (T), crossover temperatures T_c and kinetic isotope effects. For the dimer of formic acid, we find $k = 2.5 \times 10^9 \text{ s}^{-1}$ (300 K), with an associated ground-state splitting $\Delta_0 = 0.09 \text{ cm}^{-1}$. Similar to experiments with crystals of benzoic acid dimers, we obtain $T_c = 100$ K as the border between the high- and low-temperature regions of the rate constant. More than half of the hydrogenic motion occurs by quantum tunneling. The total hydrogenic motion of about 0.7 Å coincides perfectly with neutron scattering results. In contrast to all previous studies, the experimental activation energy curves can be reproduced reasonably by inclusion of tunneling from the vibrational ground state for three different isotopic species. Remaining small discrepancies from experiments with benzoic acid dimers in the coherent limit ($k \approx 10^{10} \text{ s}^{-1}$ (300 K), $\Delta_0 = 0.32 \text{ cm}^{-1}$) are explained mainly by vibrational excitation of normal modes coupled to the reaction path and the higher reaction barrier in the formic acid dimer, i.e., a difference of 1.0 kcal/mol at the B3LYP/6-31+G(d) level of theory. Closer inspection of the normal modes involved reveals that the excitation of the interdimer stretch and the OH stretch could enhance the rates and enlarge the splittings considerably by shortening the O−O distance. The reaction path with a total of 103 Hessian calculations has been obtained at the B3LYP/6-31+G(d) level of theory and corrected to a G2* reaction barrier and MP2/6-31G(d,p) frequencies at the stationary points stemming from a recent excellent benchmark study by Kim [Kim, Y. *J. Am. Chem. Soc.* **1996**, *118*, 1522−1528].

1. Introduction

Concerted proton transfer plays a major role in many phenomena in chemistry.[1−4] The synchronous double proton transfer in carboxylic acid dimers is long known and has been studied thoroughly. For a long time, experiments focused on equilibrium properties, e.g., determination of geometries of the monomers and dimers and the energetic stabilization upon dimerization using IR, Raman, and microwave spectroscopy as well as electron diffraction.[5−9] These measurements were soon followed by theoretical investigations.[10−15] Studies of the

dynamics have been possible by means of T_1-NMR spin−lattice relaxation spectroscopy. The fully symmetric double-well potential found theoretically in isolated dimers is modulated in the condensed phase of benzoic (p-toluic) acid dimers to an asymmetry of about 0.10−0.24 kcal/mol.[16−19] In these experiments, the apparent activation energy for the hydrogen transfer at room temperature has been determined to be 1.15−1.44 kcal/mol. All atoms together are dislocated by 0.69−0.80 Å during the reaction, which occurs with a frequency between 2.6×10^9 and $3.7 \times 10^{10} \text{ s}^{-1}$ for differently meta- and para-substituted benzoic and aliphatic acid dimers.[16,18,20] These results have been confirmed by inelastic neutron scattering measurements.[21,22] At low temperatures (15−50 K), the apparent activation energy goes down to 0.18−0.30 kcal/mol. Different nonaromatic carboxylic acid dimers exhibit an about 10 times slower interchange than the benzoic acid dimer.[23] In crystals of benzoic acid dimers, the deviation from centrosymmetry, i.e., the energy

(1) Jeffrey, G. A.; Saenger, W. *Hydrogen Bonding in Biological Structures*; Springer-Verlag: Berlin, 1991.

(2) Bountis, T., Ed. *Proton Transfer in Hydrogen-Bonded Systems*; NATO ASI Series 291; Plenum Press: New York, 1992.

(3) Benderskii, V. A.; Makarov, D. E.; Wight, C. A. *Chemical Dynamics at Low Temperatures*; Advances in Chemical Physics 88; John Wiley & Sons: New York, 1994.

(4) Simkin, B. Y.; Sheikhet, I. I. *Quantum Chemical and Statistical Theory of Solutions*; Ellis Horwood: London, 1995.

(5) Millikan, R. C.; Pitzer, K. S. *J. Am. Chem. Soc.* **1958**, *80*, 3515−3521.

(6) Costain, C. C.; Srivastava, G. P. *J. Chem. Phys.* **1964**, *41*, 1620−1627.

(7) Bertie, J. E.; Michaelian, K. H. *J. Chem. Phys.* **1982**, *76*, 886−894.

(8) Wilson, C. C.; Shankland, N.; Florence, A. J. *Chem. Phys. Lett.* **1996**, *253*, 103−107.

(9) Wilson, C. C.; Shankland, N.; Florence, A. J. *J. Chem. Soc., Faraday Trans.* **1996**, *92*, 5051−5057.

(10) Neuheuser, T.; Hess, B. A.; Reutel, C.; Weber, E. *J. Phys. Chem.* **1994**, *98*, 6459−6467.

(11) Qian, W.; Krimm, S. *J. Phys. Chem.* **1996**, *100*, 14602−14608.

(12) Qian, W.; Krimm, S. *J. Phys. Chem. A* **1997**, *102*, 5825−5827.

(13) Liedl, K. R.; Sekusak, S.; Mayer, E. *J. Am. Chem. Soc.* **1997**, *119*, 3782−3784.

(14) Qian, W.; Krimm, S. *J. Phys. Chem. A* **1998**, *102*, 659−667.

(15) Hage, W.; Liedl, K. R.; Hallbrucker, A.; Mayer, E. *Science* **1998**, *279*, 1332−1335.

(16) Meier, B. H.; Graf, F.; Ernst, R. R. *J. Chem. Phys.* **1982**, *76*, 767−774.

(17) Nagaoka, S.; Terao, T.; Imashiro, F.; Saika, A.; Hirota, N.; Hayashi, S. *Chem. Phys. Lett.* **1981**, *80*, 580−584.

(18) Nagaoka, S.; Terao, T.; Imashiro, F.; Saika, A.; Hirota, N. *J. Chem. Phys.* **1983**, *79*, 4694−4703.

(19) Agaki, T.; Imashiro, F.; Terao, T.; Hirota, N.; Hayashi, S. *Chem. Phys. Lett.* **1987**, *139*, 331−335.

(20) Neumann, M. A.; Craciun, S.; Corval, A.; Johnson, M. R.; Horsewill, A. J.; Benderskii, V. A.; Trommsdorff, H. P. *Ber. Bunsen.-Ges. Phys. Chem.* **1998**, *102*, 325−334.

(21) Meier, B. H.; Meyer, R.; Ernst, R. R.; Zolliker, P.; Furrer, A.; Hälg, W. *Chem. Phys. Lett.* **1983**, *103*, 169−174.

(22) Skinner, J. L.; Trommsdorf, H. P. *J. Chem. Phys.* **1988**, *89*, 897−907.

asymmetry of the double-well potential, can be removed by doping with guest heteroaromatic molecules (e.g., 10^{-4} mol/ mol of thioindigo).[24-28] The tunneling matrix element and isomerization rate are practically unaffected by the nature of these guest dyes.[20,22,25] All studied substituents of the acid dimers yield similar results, except for ortho-substituted aromatics.[18,29] The most precise determination of the tunnel matrix element by fluorescence line narrowing at $1.4-4.2$ K yields $\Delta = 0.32 \pm 0.03$ cm^{-1}, together with a zero-temperature proton tunneling rate of $k_0 \approx 2 \times 10^8$ s^{-1} in the doped crystals.[30] In mixed acetic-fluoroacetic acid dimers, the splitting was estimated from microwave rotation spectra as early as 1964 to be between 0.5 and 5.0 cm^{-1}.[6] The temperature T_c below which tunneling predominates the overbarrier mechanism is found to be between 50 and 120 K in different experimental studies, but tunneling also remains relevant in the mainly classically activated high-temperature limit.[24,31-33]

From the theoretical point of view, the experiments show that description of the dynamics by one-dimensional models is insufficient, as the exchange in the benzoic acid dimer is influenced by several normal modes.[31,34] Namely, in the first excited state of a heavy atom rocking mode, the exchange is 56 times faster than that in the ground state.[35] Also, shortening of the O—O distance by external pressure increases reaction rates.[32,36] Such an increase has been found computationally for excitation of the interdimer stretch and the CO_2 rocking mode in the formic acid dimer as enlarged tunneling splittings corresponding to increased reaction rates ($k_0 \propto \Delta^2$).[20]

Early estimates for the reaction barrier of the formic acid dimer were about 15 kcal/mol at the Hartree—Fock level of theory[37-39] and 12 kcal/mol at the MCPF and CISD levels of theory.[38,40] Today, the highest level of theory available is a G2* calculation based on MP2/6-31G(d,p) geometries and on single-point energy corrections at the MP2, MP4, and QCISD(T) level with large basis sets containing diffuse and polarization func-

tions.[41] The barrier obtained by this G2* approach is 5.20 kcal/ mol with zero-point correction and 8.94 kcal/mol without. The apparent discrepancy of the rather high theoretical and rather low experimental exchange barrier estimates was attributed to "transitions between OHO fragment vibrational levels under the action of random forces of the surrounding" and "proton tunneling promoted by the low-frequency mode excitations" in a two-dimensional study.[34] However, there are no quantitative data accounting for the difference between bare barrier height and apparent activation energy. Here, we will present the factors contributing to the lowering of the apparent activation energy in a reaction path dynamics study directly obtained from ab initio data. In contrast to other studies, our approach is full-dimensional rather than three-dimensional[40,42,43] and uses a fully ab initio calculation rather than relying on a specially parametrized semiempirical hypersurface,[41] which is important for a proper description of a wide region of the potential energy surface (PES).[44] We further studied the transfer reaction of systems containing one (HD) and two (DD) deuterons instead of the carboxylic protons. Additionally, we present the first correlated calculation of the exchange barrier in the benzoic acid dimer.

2. Method

2.1. Reaction Rate Constants. We have used variational transition state theory (VTST)[45-48] to calculate thermally averaged reaction rate constants directly from ab initio electronic structure theory.[49,50] The stationary points have been described by MP2/6-31G(d,p) frequencies and G2* energies.[41] The path of steepest descent has been evaluated in a mass-scaled coordinate system[51] employing a reduced mass of 1 amu starting from the transition state (TS) at the B3LYP/6-31+G(d) level[52-54] with the aid of the path integrator of Page—McIver[55,56] and a stepsize of $\Delta s = 0.05$ a$_o$. The Hessian has been updated at every point, resulting in a total of 103 full force constant calculations along the whole path. The information from the two different levels of theory has been combined by using a dual-level interpolation scheme based on the logarithm of ratios.[57-60] B3LYP/6-31+G(d) is able to reproduce the higher level data in a satisfactory way at the stationary points and,

(23) Horsewill, A. J.; Brougham, D. F.; Jenkinson, R. I.; McGloin, C. J.; Trommsdorff, H. P.; Johnson, M. R. *Ber. Bunsen.-Ges. Phys. Chem.* **1998**, *102*, 317−324.

(24) Clemens, J. M.; Hochstrasser, R. M.; Trommsdorf, H. P. *J. Chem. Phys.* **1984**, *80*, 1744−1753.

(25) Holtom, G. R.; Trommsdorf, H. P.; Hochstrasser, R. M. *Chem. Phys. Lett.* **1986**, *131*, 44−50.

(26) Hochstrasser, R. M.; Trommsdorff, H. P. *Chem. Phys.* **1987**, *115*, 1−6.

(27) Pierre, M.; Trommsdorff, H. P.; Hochstrasser, R. M. Optical studies of proton tunneling and relaxation in benzoic acid. In *Quantum Aspects of Molecular Motion in Solids*; Heidemann, A., Magerl, M., Prager, M., Richter, D.; Springer, T., Eds.; Proceedings in Physics 17; Springer: Berlin, 1987; pp 186−191.

(28) Rambaud, C.; Oppenländer, A.; Pierre, M.; Trommsdorff, H. P.; Vial, J.-C. *Chem. Phys.* **1989**, *136*, 335−347.

(29) Heuer, A.; Haeberlen, U. *J. Chem. Phys.* **1991**, *95*, 4201−4214.

(30) Oppenländer, A.; Rambaud, C.; Trommsdorff, H. P.; Vial, J. C. *Phys. Rev. Lett.* **1989**, *63*, 1432−1435.

(31) Stöckli, A.; Meier, B. H.; Kreis, R.; Meyer, R.; Ernst, R. R. *J. Chem. Phys.* **1990**, *93*, 1502−1520.

(32) Horsewill, A. J.; McDonald, P. J.; Vijayaraghavan, D. *J. Chem. Phys.* **1994**, *100*, 1889−1894.

(33) Brougham, D. F.; Horsewill, A. J.; Jenkinson, R. I. *Chem. Phys. Lett.* **1997**, *272*, 69−74.

(34) Sakun, V. P.; Vener, M. V.; Sokolov, N. D. *J. Chem. Phys.* **1996**, *105*, 379−387.

(35) Meyer, R.; Ernst, R. R. *J. Chem. Phys.* **1990**, *93*, 5518−5532.

(36) Brougham, D. F.; Horsewill, A. J.; Ikram, A.; Ibberson, R. M.; McDonald, P. J.; Pinter-Krainer, M. *J. Chem. Phys.* **1996**, *105*, 979−982.

(37) Graf, F.; Meyer, R.; Ha, T.-K.; Ernst, R. R. *J. Chem. Phys.* **1992**, *75*, 2914−2918.

(38) Hayashi, S.; Umemura, J.; Kato, S.; Morokuma, K. *J. Phys. Chem.* **1984**, *88*, 1330−1334.

(39) Chang, Y.-T.; Yamaguchi, Y.; Miller, W. H.; Schaefer, H. F., III. *J. Am. Chem. Soc.* **1987**, *109*, 7245−7253.

(40) Shida, N.; Barbara, P. F.; Almlöf, J. *J. Chem. Phys.* **1991**, *94*, 3633−3643.

(41) Kim, Y. *J. Am. Chem. Soc.* **1996**, *118*, 1522−1528.

(42) Shida, N.; Almlöf, J.; Barbara, P. F. *J. Phys. Chem.* **1991**, *95*, 10457−10464.

(43) Benderskii, V. A.; Grebenshchikov, S. Y.; Makarov, D. E.; Vetoshkin, E. V. *Chem. Phys.* **1994**, *185*, 101−112.

(44) Loerting, T.; Liedl, K. R.; Rode, B. M. *J. Am. Chem. Soc.* **1998**, *120*, 404−412.

(45) Truhlar, D. G.; Isaacson, A. D.; Garrett, B. C. Generalized Transition State Theory. In *Theory of Chemical Reaction Dynamics*; Baer, M., Ed.; CRC Press: Boca Raton, FL, 1985; pp 65−137.

(46) Kreevoy, M. M.; Truhlar, D. G. Transition State Theory. In *Investigation of Rates and Mechanisms of Reactions*; Bernasconi, C. F., Ed.; John Wiley & Sons: New York, 1986; pp 13−95.

(47) Tucker, S. C.; Truhlar, D. G. Dynamical Formulation of Transition State Theory: Variational Transition States and Semiclassical Tunneling. In *New Theoretical Concepts for Understanding Organic Reactions*; Bertrán, J., Csizmadia, I. G., Eds.; NATO ASI Series C 267; Kluwer: Dordrecht, The Netherlands, 1989; pp 291−346.

(48) Truhlar, D. G.; Garrett, B. C.; Klippenstein, S. J. *J. Phys. Chem.* **1996**, *100*, 12771−12800.

(49) Baldridge, K. K.; Gordon, M. S.; Steckler, R.; Truhlar, D. G. *J. Phys. Chem.* **1989**, *93*, 5107−5119.

(50) Truhlar, D. G. Direct Dynamics Method for the Calculation of Reaction Rates. In *The Reaction Path in Chemistry: Current Approaches and Perspectives*; Heidrich, D., Ed.; Kluwer: Dordrecht, The Netherlands, 1995; pp 229−255.

(51) Miller, W. H.; Handy, N. C.; Adams, J. E. *J. Chem. Phys.* **1980**, *72*, 99−112.

(52) Becke, A. D. *J. Chem. Phys.* **1993**, *98*, 5648−5652.

(53) Märker, C.; Schleyer, P. v. R.; Liedl, K. R.; Ha, T.-K.; Quack, M.; Suhm, M. A. *J. Comput. Chem.* **1997**, *18*, 1695−1719.

(54) Becke, A. D. *J. Chem. Phys.* **1997**, *107*, 8554−8560.

(55) Page, M.; McIver, J. W., Jr. *J. Chem. Phys.* **1988**, *88*, 922−935.

(56) Melissas, V. S.; Truhlar, D. G.; Garrett, B. C. *J. Chem. Phys.* **1992**, *96*, 5758−5772.

therefore, is suitable for the interpolation. The B3LYP/6-31+G(d) barrier height of 8.39 kcal/mol is in excellent agreement with the higher G2* level of theory.

The classical VTST rate constant has been corrected semiclassically to describe nonclassical barrier penetration and reflection. Three different corrections have been employed, namely for zero- (ZCT), small- (SCT), and large-curvature tunneling (LCT). In the zero-curvature limit, tunneling occurs directly along the steepest-descent minimum energy path (MEP). However, a reduction of this tunneling length, i.e., corner cutting, is possible on the concave side of this path.[61−63] In the CD-SCSAG method (SCT), this effect is described by appropriate lowering of the effective reduced mass for motion along the MEP.[49,61] On the other hand, the LCG3 correction (LCT)[64−69] takes into account that direct corner-cutting can as well occur far away from the steepest-descent path on the so-called reaction swath,[44,70,71] i.e., the region on the concave side of the reaction path extending beyond the transverse vibrational turning points and/or beyond the local radius of curvature. Motions over the swath are initiated by vibrations orthogonal to the MEP as well as parallel to it. Sudden tunneling along straight line paths over the swath may provide the most effective tunneling mechanism for a system of high reaction path curvature, e.g., the bimolecular transfer of a light atom between two heavy atoms. The effective potential for tunneling over the adiabatic part of the swath is obtained from Hessian calculations on the MEP, whereas the effective potentials for nonadiabatic regions (those beyond the vibrational turning points and/or the local radius of curvature) are obtained from single-point energy calculations along those portions of the path.[45,66,67] We have used the interface Gaussrate[72] between Polyrate[73] and Gaussian94.[74]

2.2. Tunneling Splitting. For further comparison to experiment, the tunneling splitting Δ_0 has been estimated from the data of the reaction path calculation. Namely, the ground-state tunneling probability P^Q at zero-temperature and the equilibrium reaction coordinate double-well potential frequency ω_0 can be utilized for this purpose:[71,75,76]

$$\Delta_0 = \left(\frac{\omega_0}{\pi}\right)\sqrt{P^Q}$$

Therefore, the zero-level tunneling splitting is related to the low-temperature limit of the tunneling correction. It is hence temperature-independent and can be compared directly with molecular beam experiments, which involve measuring pure transitions between two well-defined quantum states. These "rough estimates" have been quite successfully used to predict ground-state splittings Δ_0.[77−79] Data for the transfer in $(HF)_2$ obtained from reaction path calculations (0.44 and 0.61 cm^{-1})[80] are comparable to accurate quantal calculations (0.43−0.66 cm^{-1})[81,82] in predicting the experimental value (0.66 cm^{-1}).[83] As the sudden straight line paths are expected to be the most probable reaction mechanism yielding the highest rates, the LCG3 tunneling probability has been used for this estimate. However, if more precise information, such as mode-specific splittings, are desired, other approaches to obtain tunneling-splittings have to be applied.[76,84−91]

3. Results

3.1. Reaction Rate and Mechanism. As can be seen in Figure 1, the highest tunneling corrections stem from the direct corner-cutting (LCT) approximation, which is reasonable for the mass combination of the transfer studied. The reaction thus takes place by first following the MEP starting from the minima in order to decrease the O−O distance. When the system has reached an orientation where the potential in the swath is favorable, it crosses the dividing surface in a straight manner by directly following the OH stretch direction. Typically, this orientation is near the TS at high temperatures (i.e., O−O distance reduction of nearly 0.3 Å) and near the minimum structure at low temperatures (i.e., O−O distance reduction of less than 0.1 Å). The representative tunneling energy is 1.0 and 2.0 kcal/mol below the saddle at 300 and 100 K, respectively. A similar mechanism of a preliminary hydrogen bond compression has also been found in some other systems showing multiple hydrogen transfers.[92−95] In comparison to the LCT rate constants obtained directly from VTST at the AM1-SRP level of theory,[41] our predictions are higher by 2 orders of magnitude at 200 K and one at 300 K as predicted qualitatively previously.[44] The difference is, on the one hand, due to the much steeper ridge of the reaction swath[44,71,96] at the AM1-SRP level and, on the other hand, due to the AM1-SRP barrier higher by 0.7 kcal/mol.

(57) Hu, W. P.; Liu, Y. P.; Truhlar, D. G. *J. Chem. Soc., Faraday Trans.* **1994**, *90*, 1715−1725.

(58) Corchado, J. C.; Espinosa-Garcia, J.; Hu, W.-P.; Rossi, I.; Truhlar, D. G. *J. Phys. Chem.* **1995**, *99*, 687−694.

(59) Nguyen, K. A.; Rossi, I.; Truhlar, D. G. *J. Chem. Phys.* **1995**, *103*, 5522−5530.

(60) Chuang, Y.-Y.; Truhlar, D. G. *J. Phys. Chem. A* **1997**, *101*, 3808−3814.

(61) Skodje, R. T.; Truhlar, D. G.; Garrett, B. C. *J. Phys. Chem.* **1981**, *85*, 3019−3023.

(62) Skodje, R. T.; Truhlar, D. G.; Garrett, B. C. *J. Chem. Phys.* **1982**, *77*, 5955−5976.

(63) Liu, Y.-P.; Lynch, G. C.; Truong, T. N.; Lu, D.-h.; Truhlar, D. G.; Garrett, B. C. *J. Am. Chem. Soc.* **1993**, *115*, 2408−2415.

(64) Garrett, B. C.; Truhlar, D. G. *J. Chem. Phys.* **1983**, *79*, 4931−4938.

(65) Lynch, G. C.; Truhlar, D. G.; Garrett, B. C. *J. Chem. Phys.* **1989**, *90*, 3102−3109.

(66) Garrett, B. C.; Joseph, T.; Truong, T. N.; Truhlar, D. G. *Chem. Phys.* **1989**, *136*, 271−283.

(67) Liu, Y.-P.; Lu, D.-h.; Gonzalez-Lafont, A.; Truhlar, D. G.; Garrett, B. C. *J. Am. Chem. Soc.* **1993**, *115*, 7806−7817.

(68) Taketsugu, T.; Hirao, K. *J. Chem. Phys.* **1997**, *107*, 10506−10514.

(69) Schwieters, C. D.; Voth, G. A. *J. Chem. Phys.* **1998**, *108*, 1055−1062.

(70) Truhlar, D. G.; Gordon, M. S. *Science* **1990**, *249*, 491−498.

(71) Loerting, T.; Liedl, K. R.; Rode, B. M. *J. Chem. Phys.* **1998**, *109*, 2672−2679.

(72) Corchado, J. C.; Coitino, E. L.; Chuang, Y.-Y.; Truhlar, D. G. *Gaussrate7.4.1*; University of Minnesota, Minneapolis, MN, 1997.

(73) Steckler, R.; Chuang, Y.-Y.; Coitino, E. L.; Fast, P. L.; Corchado, J. C.; Hu, W.-P.; Liu, Y.-P.; Lynch, G. C.; Nguyen, K. A.; Jackels, C. F.; Gu, M. Z.; Rossi, I.; Clayton, S.; S.Melissas, V.; Garrett, B. C.; Isaacson, A. D.; Truhlar, D. G. *POLYRATE-version 7.2*; University of Minnesota, Minneapolis, MN, 1997.

(74) Frisch, M. J.; Trucks, G. W.; Schlegel, H. B.; Gill, P. M. W.; Johnson, B. G.; Robb, M. A.; Cheeseman, J. R.; Keith, T. A.; Petersson, G. A.; Montgomery, J. A.; Raghavachari, K.; Al-Laham, M. A.; Zakrzewski, V. G.; Ortiz, J. V.; Foresman, J. B.; Cioslowski, J.; Stefanov, B. B.; Nanayakkara, A.; Challacombe, M.; Peng, C. Y.; Ayala, P. Y.; Chen, W.; Wong, M. W.; Andres, J. L.; Replogle, E. S.; Gomperts, R.; Martin, R. L.; Fox, D. J.; Binkley, J. S.; Defrees, D. J.; Baker, J.; Stewart, J. P.; Head-Gordon, M.; Gonzalez, C.; Pople, J. A. *Gaussian 94, Revision D.1*; Gaussian, Inc., Pittsburgh, PA, 1995.

(75) Smedarchina, Z.; Fernandez-Ramos, A.; Rios, M. A. *J. Chem. Phys.* **1997**, *106*, 3956−3964.

(76) Fernández-Ramos, A.; Smedarchina, Z.; Zgierski, M. Z.; Siebrand, W. *J. Chem. Phys.* **1998**, *109*, 1004−1013.

(77) Smedarchina, Z.; Caminati, W.; Zerbetto, F. *Chem. Phys. Lett.* **1995**, *237*, 279−285.

(78) Smedarchina, Z.; Siebrand, W.; Zgierski, M. Z. *J. Chem. Phys.* **1995**, *103*, 5326−5334.

(79) Smedarchina, Z.; Siebrand, W.; Zgierski, M. Z. *J. Chem. Phys.* **1996**, *104*, 1203−1212.

(80) Miller, W. H. *J. Phys. Chem.* **1979**, *83*, 960−963.

(81) Hancock, G. C.; Rejto, P.; Steckler, R.; Brown, F. B.; Schwenke, D. W.; Truhlar, D. G. *J. Chem. Phys.* **1986**, *85*, 4997−5003.

(82) Hancock, G. C.; Truhlar, D. G. *J. Chem. Phys.* **1989**, *90*, 3498−3505.

(83) Volobuev, Y.; Necoechea, W. C.; Truhlar, D. G. *J. Phys. Chem. A* **1997**, *101*, 3045−3048.

(84) Makri, N.; Miller, W. H. *J. Chem. Phys.* **1987**, *86*, 1451−1457.

(85) Wales, D. J. *J. Am. Chem. Soc.* **1993**, *115*, 11191−11201.

(86) Duncan, W. T.; Truong, T. N. *J. Chem. Phys.* **1995**, *103*, 9642−9652.

(87) Gregory, J. K.; Clary, D. C. *J. Chem. Phys.* **1995**, *102*, 7817−7829.

(88) Paz, J. J.; Moreno, M.; Lluch, J. M. *J. Chem. Phys.* **1995**, *103*, 353−359.

(89) Benderskii, V. A.; Vetoshkin, E. V.; Grebenshchikov, S. Y.; von Laue, L.; Trommsdorff, H. P. *Chem. Phys.* **1997**, *219*, 119−142.

(90) Benderskii, V. A.; Vetoshkin, E. V.; von Laue, L.; Trommsdorff, H. P. *Chem. Phys.* **1997**, *219*, 143−160.

(91) Klochikin, V. L.; Trakhtenberg, L. I. *Chem. Phys. Lett.* **1998**, *285*, 34−40.

(92) Meschede, L.; Limbach, H. H. *J. Phys. Chem.* **1991**, *95*, 10267−10280.

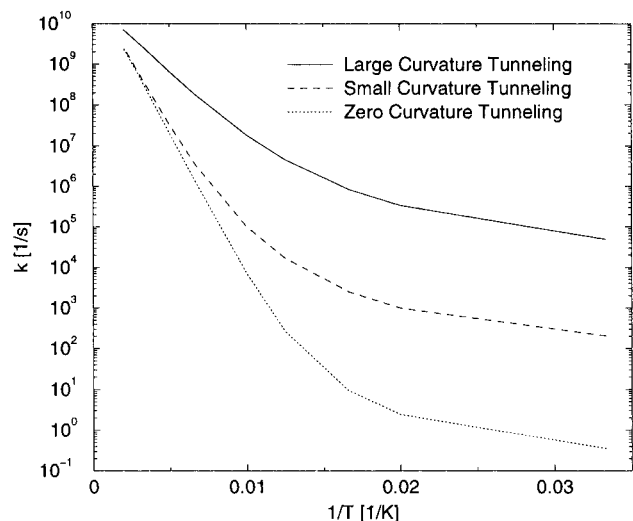(93) Scherer, G.; Limbach, H. H. *J. Am. Chem. Soc.* **1994**, *116*, 1230−1239.

Figure 1. Reaction rate constants for the concerted proton exchange in $(HCOOH)_2$ at the MP2///B3LYP level employing different tunneling corrections.
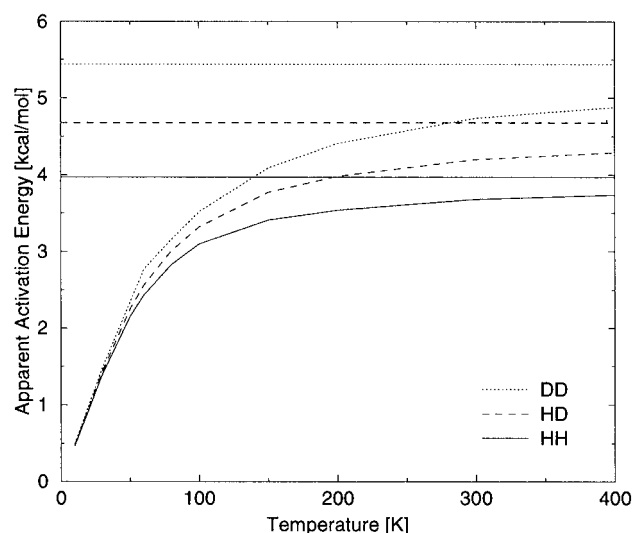

Figure 2. Isotope effect on apparent activation energy of intermolecular proton exchange in $(HCOOH)_2$ [HH], (HCOOH)(HCOOD) [HD], and $(HCOOD)_2$ [DD] at the B3LYP/6-31+G(d) level with small curvature tunneling correction from ground state. For comparison, the zero-point corrected barriers are shown (straight lines).

3.2. Importance of Tunneling up to Room Temperature.

The crossover temperature T_c between the high- and low-temperature regimes is found to be between 70 and 100 K from the change between the two linear regions in the Arrhenius plot. Already the ZCT approximation provides a good estimate for T_c, although the intermediate region is broader compared to the LCT result. Especially the latter compares very well with the experimental curves.[24,31−33] Below T_c, tunneling predominates clearly, as can be seen from the small amount of heavy atom movement. Above T_c, tunneling still plays a major role. Namely, we find a proton tunneling distance of more than 0.4 Å at the representative LCT path (300 K). A similar result has been obtained by Kim.[41] The total displacement between the two minima of 0.63 Å compares very well with the recent neutron

(94) Aguilar-Parrilla, F.; Klein, O.; Elguero, J.; Limbach, H. H. *Ber. Bunsen.-Ges. Phys. Chem.* **1997**, *101*, 889−901.

(95) Benedict, H.; Limbach, H.-H.; Wehlan, M.; Fehlhammer, W.-P.; Golubev, N. S.; Janoschek, R. *J. Am. Chem. Soc.* **1998**, *120*, 2939−2950.

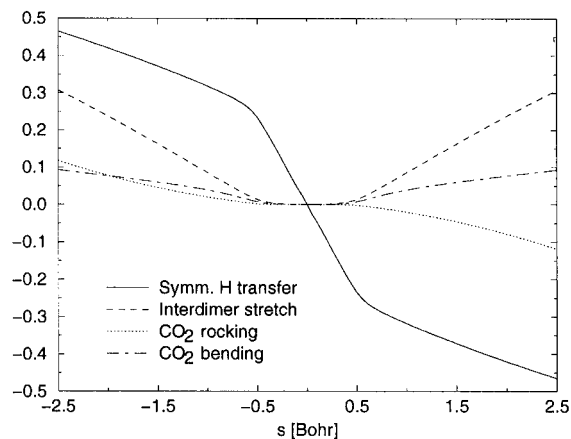(96) Liedl, K. R.; Sekusak, S.; Kroemer, R. T.; Rode, B. M. *J. Phys. Chem. A* **1997**, *101*, 4707−4716.

Figure 3. Minimum energy path for the concerted hydrogen exchange in $(HCOOH)_2$ in D_{2h} (TS) normal-mode basis (see Figure 5). All other normal modes exhibit coefficients lower than 0.05.
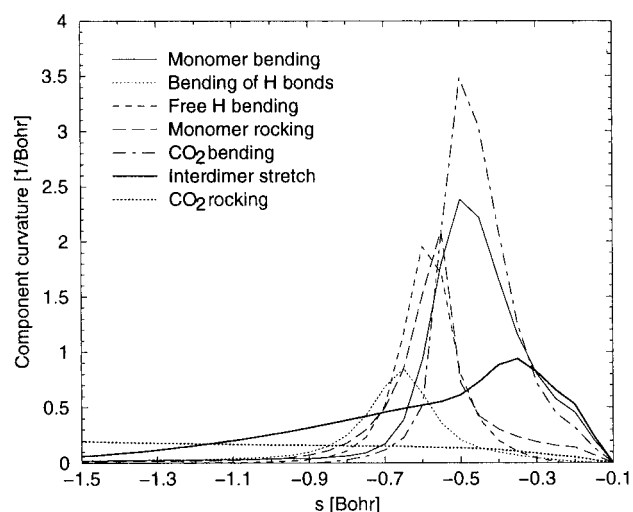

Figure 4. MP2///B3LYP curvature couplings to the minimum energy path.

Table 1. Frequency (cm^{-1}), Reduced Mass (amu), and Irreducible Representation of the Normal Modes Important for the HH Transfer at the Transition State As Predicted from B3LYP/6-31+G(d)

description	wavelength	μ	symmetry
monomer rocking	1751	4.1	B_{3g}
bending of H bonds	1639	1.1	A_g
free H bending	1406	1.1	B_{3g}
monomer bending	1400	6.6	A_g
CO_2 bending	737	6.6	A_g
interdimer stretch	491	9.2	A_g
CO_2 rocking	231	12.5	B_{3g}
symm. H transfer	1324i	1.1	B_{3g}

scattering result of 0.686 Å.[20] More than half of the total hydrogenic motion occurs, therefore, in the classically forbidden tunneling region, even at ambient temperature.

The associated tunneling splitting is estimated to be $\Delta_0 = 0.09$ cm^{-1}. This is an order of magnitude higher than the one found employing a three-dimensional PES.[40] It has been suggested that the adiabatical treatment of the strongly and linearly coupled low-frequency CO_2 rocking mode[20,37,89,90] is the reason for the small splitting found in this study.[43,89] However, comparing the employed MCPF barrier of 12.0 kcal/mol with the G2* barrier of 8.9 kcal/mol,[41] the difference rather seems to emerge from the too-high barrier. Other low-dimensional studies yielded splittings of 1.8 (Makri and Miller[97])

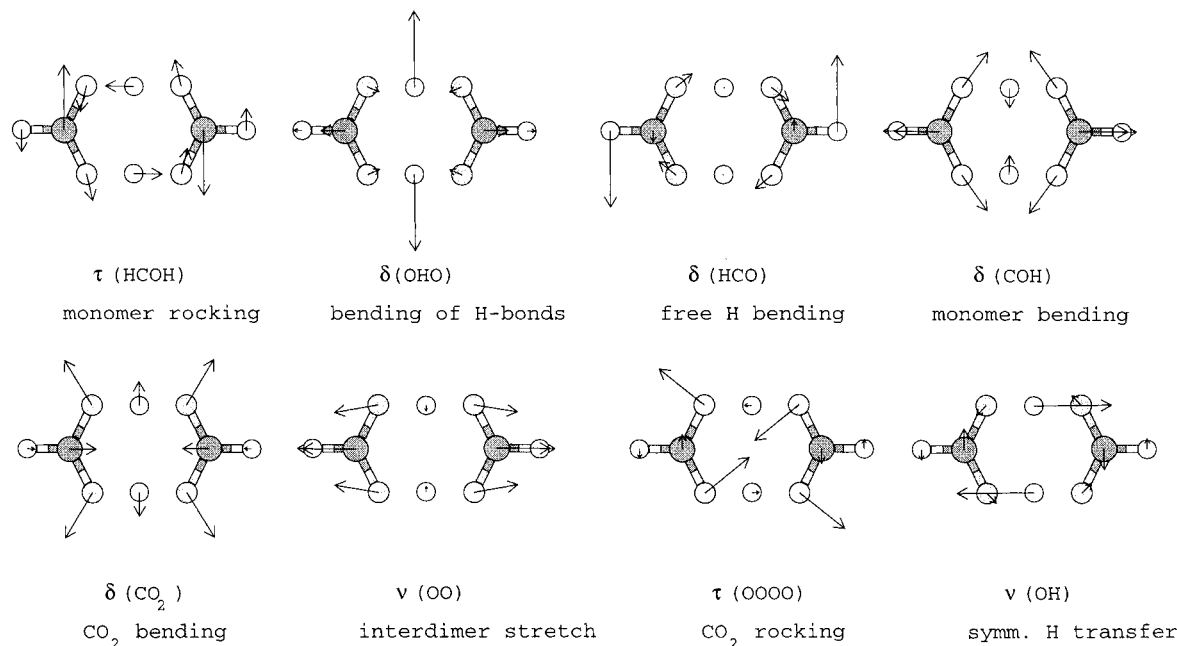(97) Makri, N.; Miller, W. H. *J. Chem. Phys.* **1989**, *91*, 4026−4036.

Figure 5. Normal modes of the transition state participating actively in the concerted proton transfer in the formic acid dimer.

and 0.3 cm^{-1} (Chang et al.[39]) for the ground state but seem to suffer from neglecting skeletal motion and thus give an unphysical low effective mass.

3.3. Isotopic Substitution. It has been pointed out earlier[64,65,76] that LCT isotope effects do not compare very well with the experiments. Obviously, they are suffering from the fact that the straight line paths are poor approximations for the deuterated species. However, in the small-curvature regime, we find kinetic isotope effects that compare very favorably with the experiment.[16,18,31] While the predicted curve for the ratio of k(HH) to k(HD) approaches $2^{1/2}$ at high temperatures (e.g., 2.2 at 380 K), we obtain higher values at lower temperatures due to enhanced tunneling. A similar behavior is found for the ratio of k(HD) to k(DD), with the exception that it starts from lower values at low temperatures and drops more slowly to $2^{1/2}$ upon increasing the temperature.

The stronger increase of OH vs OD stretching frequencies in the minimum structure compared to the TS causes an increase of the zero-point corrected B3LYP/6-31+G(d) barrier from 3.97 to 4.68 and 5.44 kcal/mol from the HH to the HD and DD species, respectively.

3.4. Apparent Activation Energy. The reduction of these zero-point corrected barriers due to tunneling is shown in Figure 2. Earlier attempts to reproduce the experimental results[16,18−20] suffered from uncorrelated barriers, uncompletely optimized transition states showing too long O−O distances, and the omission of tunneling.[37−39,98] The curves given here are in considerably better agreement but are still slightly higher than the experimental results, i.e., 1.4 kcal/mol at room temperature.[16,18,31] We propose that some further effects account for the remaining small discrepancy.

3.4.1. Correlated Barrier in the Benzoic Acid Dimer. First, the barrier for the benzoic acid dimer (BAD) is lower than that for the formic acid dimer (FAD). For the BAD, the barrier seemed to be lower by about 2 kcal/mol judging from calculations not taking into account electron correlation, which was unfortunately the highest level of theory available in the literature for this system of 128 electrons.[98] Thus, we have performed an improved calculation of the barrier for the proton

exchange in the BAD, which is, to the best of our knowledge, the first one taking into account electron correlation. Namely, at the B3LYP/6-31+G(d) level of theory, the barrier for concerted proton exchange in the BAD amounts to 7.40 kcal/mol. This implies a barrier reduction of 0.99 kcal/mol by the phenyl substituent in comparison to the FAD. Besides this lower theoretical prediction of the BAD barrier, a presumable underestimation of the experimental ground-state barrier of the BAD[31] further contributes to a better matching between the theoretical (FAD) and experimental (BAD) activation energy plots.

Additionally, incoherent transfer is important for some experimental results. Our theoretical study focuses on the coherent transfer that has been realized experimentally through the doped systems of benzoic acid dimers. The effects arising on the transition to incoherent transfer are not the subject of the present study. However, a more complete understanding of dynamics in the undoped condensed phase is an active field of research.[99−103]

3.4.2. Vibrational Excitation. Finally, excitation of vibrations due to the thermal bath of neighboring molecules can lead to a considerable increase in the rate constants.[20,31,34,35,90] It is thus necessary to investigate the normal modes participating in the reaction in order to identify the modes accelerating the reaction on excitation. Therefore, we have recalculated the MEP in another coordinate system using the 24 vectors of normal mode vibrations at the transition state as basis. The multiples of each vector needed to reach a specific point on the MEP from the TS are called coefficients.[44,104] Analyzing these coefficients along the whole MEP, we can assert that mainly four vectors (i.e., normal modes) are relevant for the proton exchange. The coefficients of these important normal modes are depicted in Figure 3. We thus agree with a previous study[89] that at least a four-dimensional treatment is necessary for a correct description

(98) Nagaoka, S.; Hirota, N.; Matsushita, T.; Nishimoto, K. *Chem. Phys. Lett.* **1982**, *92*, 498−502.

(99) Scheurer, C.; Saalfrank, P. *Chem. Phys. Lett.* **1995**, *245*, 201−208.
(100) Scheurer, C.; Saalfrank, P. *J. Chem. Phys.* **1995**, *104*, 2869−2882.
(101) Turi, L. *J. Phys. Chem.* **1996**, *100*, 11285−11291.
(102) Sundholm, D.; Sundberg, M. R.; Uggla, R. *J. Phys. Chem. A* **1998**, *102*, 7137−7142.
(103) Antoniou, D.; Schwartz, S. D. *J. Chem. Phys.* **1998**, *109*, 2287−2293.
(104) Liedl, K. R.; Kroemer, R. T.; Rode, B. M. *Chem. Phys. Lett.* **1995**, *246*, 455−462.

of the dynamics. These four dimensions are the synchronous hydrogen transfer (OH stretch), interdimer stretch, CO_2 rocking, and CO_2 bending modes (cf. Figure 5). The OH stretch mode contributes to the reaction for the whole process, whereas the other three modes do not participate near the TS (within ± 0.5 a_0); i.e., they are just assisting prior to the actual hydrogen transfer by reducing the O−O distance. The rate of transfer is, therefore, strongly influenced by excitation of these modes. Raising the OH stretch from the ground state to the first excited state leads to a shortening of the O−O distance by 0.073 Å and an increase of the tunneling splitting by a factor of 10−100, as predicted from spectra of carboxylic acid bimolecules.[6] In contrast to a previous study, we find that motions of symmetry other than A_g or B_{3g}, such as the asymmetric hydrogen-transfer coordinate (B_{1g}), do not contribute to the coherent reaction.[40] The corresponding coefficients are perfectly zero, while other A_g or B_{3g} modes show contributions lower than 0.05 along the whole path. However, the representative LCT path is in qualitative agreement with the most probable path (MPP) found by Shida et al.[40,42]

The curvature couplings of the various modes to the intrinsic reaction coordinate are depicted in Figure 4. The same modes as in Figure 3 are found to be relevant. The OH stretch mode is missing, as it is the transfer coordinate by itself. The remaining modes are essentially the same as those found by Benderskii et al.[89] These modes have only small nonzero normal-mode coefficients, but the coupling constant becomes as large as 2.4 a_o^{-1} for the monomer rocking. Most of the modes show maximal coupling between 0.3 and 0.7 a_o, where also the gradient reaches a maximum. Only the coupling of the CO_2 rocking mode increases continuously toward the entrance channel of the reaction. Excitation of modes coupled to the reaction path enhances the reaction rate due to an increased energy flow to the reaction coordinate.[45,51,86,105] Therefore, the CO_2 rocking is perfectly suitable for accelerating the transfer in its vibrationally excited states in the entrance channel. The other modes can enhance the reaction in later stages of the reaction, even in the part of the reaction where direct corner cutting occurs, because the modes of Figure 4 are as well coupled to the LCT paths. The characterization of all relevant normal modes is shown in Table 1 and Figure 5.

4. Discussion

We have presented transition-state calculations for the reaction rate constant of the double-proton-transfer reaction in the formic acid dimer. The study is full-dimensional and does not need any fit to an analytical potential. Instead, it directly calculates all information from B3LYP/6-31+G(d) and uses the barrier height from G2* and frequencies from MP2/6-31G(d,p) calculations.[41] The results of studies using only hydrogenic motion coordinates should be seen with care. The effective mass for most of the relevant vibrations (cf. Table 1) is considerably larger than 1 amu. Reducing the dimensionality of the problem by omitting these normal modes will lead to overestimated tunneling splittings and rates. An eight-dimensional description of the formic acid dimer involving the modes shown in Figure 5 is sufficient in any case, but it could be possible to reduce the problem to four dimensions. Upon considering that more than half of the hydrogenic motion occurs by quantum tunneling, an incomplete treatment of tunneling and corner-cutting must lead to bad estimates of rate constants and apparent activation energy plots.[38] By allowing corner-cutting, we remove the vast

deviation in apparent activation energy between experiment and theory. Inclusion of only the vibrational ground states of the educt yields a reduction of the apparent activation energy to 3.5 kcal/mol at room temperature. We surmise that the remaining difference from the experimental value of 1.4 kcal/mol in the benzoic acid dimer[16,18,31] is due to the ground-state approximation along the MEP, which precludes excitation of normal modes coupled to the reaction path, and the barrier in the formic acid dimer, higher by 1.0 kcal/mol at the B3LYP/6-31+G(d) level of theory.

The basis transformation coefficients and curvature couplings indicate that selective excitation of some low-frequency modes, especially the interdimer stretch and CO_2 rocking, and the OH stretch could enhance the exchange rate by shortening the reaction distance. Excitation of low-frequency modes can lead to an enlargement of the ground-state splittings by more than 15 times, which corresponds to a k_0 larger by more than 225 times.[20] The problem of subpicosecond intramolecular vibrational energy redistribution (IVR)[106−108] could hinder this enhancement in certain cases. However, it has been shown experimentally that a reduction of the O−O distance by either exciting the OH stretch mode into the first vibrational state (0.073 Å)[6] or by applying pressure to the system (0.03 Å) yields an increase by a factor of 10 in the rate.[32,36] These experiments confirm that vibrational excitation is responsible for a quantitative reproduction of experimental rate constants and tunneling splittings. Due to additional "imaginary" frequencies in the neighborhood of the TS, our calculations further suggest not only that the splittings and rates can be modulated by selectively exciting vibrations[34,109] but also that the reaction mechanism can possibly be directed toward an asynchronous transfer by altering reaction conditions. At the Hartree−Fock level of theory in a dielectric medium of $\epsilon = 78.4$ intermediates for asynchronous proton transfer already have been identified.[110] The kinetic isotope effect compares favorably to the experiments in the SCT approximation but rather unsatisfactorily at the LCT level. It has been recognized by other authors that a search for the least-action path between the MEP and LCT paths further improves results.[64,65,76] Nevertheless, the newest VTST approaches to the kinetic isotope effects of hydrogen-transfer reactions are very successful, even without calculating separate reaction paths for the different isotopic species[111−116] and thus provide a promising perspective for future calculations. We hope that we have pointed out directions for new experimental work and for further studies accounting properly for the excitation of vibrations and the environment in the condensed phase.

(105) Dunning, T. H.; Bowman, J. M.; Schatz, G. C.; Wagner, A. F.; Harding, L. B. *Science* **1988**, *240*, 453−459.

(106) Stuchebrukhov, A. A.; Marcus, R. A. *J. Chem. Phys.* **1993**, *98*, 6044−6061.

(107) Schranz, H. W.; Collins, M. A. *J. Chem. Phys.* **1993**, *98*, 1132−1148.

(108) Schranz, H. W.; Collins, M. A. *J. Chem. Phys.* **1994**, *101*, 307−321.

(109) Sato, N.; Iwata, S. *J. Chem. Phys.* **1988**, *89*, 2932−2937.

(110) Lim, J.-H.; Lee, E. K.; Kim, Y. *J. Phys. Chem.* **1997**, *101*, 2233−2239.

(111) Villa, J.; Truhlar, D. G. *Theor. Chim. Acta* **1997**, *97*, 317−323.

(112) Roberto-Neto, O.; Coitiño, E. L.; Truhlar, D. G. *J. Phys. Chem. A* **1998**, *102*, 4568−4578.

(113) Corchado, J. C.; Coitiño, E. L.; Chang, Y.-Y.; Fast, P. L.; Truhlar, D. G. *J. Phys. Chem. A* **1998**, *102*, 2424−2438.

(114) González-Lafont, A.; Villá, J.; Lluch, J. M.; Bertrán, J.; Steckler, R.; Truhlar, D. G. *J. Phys. Chem. A* **1998**, *102*, 3420−3428.

(115) Fast, P. L.; Truhlar, D. G. *J. Phys. Chem.* **1998**, *109*, 3721−3729.

(116) Fast, P. L.; Corchado, J. C.; Truhlar, D. G. *J. Chem. Phys.* **1998**, in press.